AFRL-AFOSR-JP-TR-2018-0010

144090 - Science & Emerging Technology of 2D Atomic Layered Materials and Devices

Masayoshi Tonouchi
Osaka University

01/31/2018
Final Report

Air Force Research Laboratory
AF Office Of Scientific Research (AFOSR)/ IOA
Arlington, Virginia 22203
Air Force Materiel Command

REPORT DOCUMENTATION PAGE

Form Approved
OMB No. 0704-0188

1. REPORT DATE *(DD-MM-YYYY)*	2. REPORT TYPE	3. DATES COVERED *(From - To)*
01-02-2018	Final	19 Nov 2014 to 18 Nov 2017

4. TITLE AND SUBTITLE
144090 - Science & Emerging Technology of 2D Atomic Layered Materials and Devices

5a. CONTRACT NUMBER

5b. GRANT NUMBER
FA2386-15-1-0004

5c. PROGRAM ELEMENT NUMBER
61102F

6. AUTHOR(S)
Masayoshi Tonouchi

5d. PROJECT NUMBER

5e. TASK NUMBER

5f. WORK UNIT NUMBER

7. PERFORMING ORGANIZATION NAME(S) AND ADDRESS(ES)
Osaka University
8-1 MIHOGAOKA IBARAKI
OSAKA, 567-0047 JP

8. PERFORMING ORGANIZATION REPORT NUMBER

9. SPONSORING/MONITORING AGENCY NAME(S) AND ADDRESS(ES)
AOARD
UNIT 45002
APO AP 96338-5002

10. SPONSOR/MONITOR'S ACRONYM(S)
AFRL/AFOSR IOA

11. SPONSOR/MONITOR'S REPORT NUMBER(S)
AFRL-AFOSR-JP-TR-2018-0010

12. DISTRIBUTION/AVAILABILITY STATEMENT
A DISTRIBUTION UNLIMITED: PB Public Release

13. SUPPLEMENTARY NOTES

14. ABSTRACT
Atomically thin material such as graphene is known to be extremely susceptible to its environment, including defects and phonons in the substrate on which it is placed as well as gas molecules that surround it. Therefore, it is necessary to develop novel methods capable of quantitatively measuring the dynamics of adsorption and desorption of molecules on graphene and the influence of those phenomena on the electronic state of graphene. In this project, the research team has developed temperature-programmed terahertz (THz) emission microscopy that can map the dynamics of absorption and desorption of absorbed molecules on two-dimensional materials and determine the adsorption energy of the molecules. They obtained the first experimental value of the adsorption energy of locally physisorbed oxygen molecules on graphene and WS2. Moreover, the team has developed novel THz time domain spectroscopy (THz-TDS) with parallel-plate waveguides (PPWG) to study atomically thin materials. They demonstrate that a low carrier density graphene, which induces less than 1% absorption in conventional THz-TDS, exhibits ~30% absorption in our PPWG-based system and the signal to noise ratio is dramatically improved.

15. SUBJECT TERMS
atomic

16. SECURITY CLASSIFICATION OF:			17. LIMITATION OF ABSTRACT	18. NUMBER OF PAGES	19a. NAME OF RESPONSIBLE PERSON
a. REPORT	b. ABSTRACT	c. THIS PAGE			MAH, MISOON
Unclassified	Unclassified	Unclassified	SAR	20	19b. TELEPHONE NUMBER *(Include area code)* 703-696-9562

Standard Form 298 (Rev. 8/98)
Prescribed by ANSI Std. Z39.18

Final Report for AOARD Grant FA2386-15-1-0004

"**2D Materials and Devices Beyond Graphene Science & Emerging Technology of 2D Atomic Layered Materials and Devices**"

30 January, 2018

Name of Principal Investigators (PI and Co-PIs):Masayoshi Tonouchi

- e-mail address : tonouchi@ile.osaka-u.ac.jp
- Institution : Osaka University
- Mailing Address : 2-6 Yamadaoka, Suita, Osaka 565-0871
- Phone : 81-6-6879-7983
- Fax : 81-6-6879-7984

Period of Performance: 11/19/2014 – 11/18/2017

Abstract

Atomically thin material such as graphene is known to be extremely susceptible to its environment, including defects and phonons in the substrate on which it is placed as well as gas molecules that surround it. Therefore, it is necessary to develop novel methods capable of quantitatively measuring the dynamics of adsorption and desorption of molecules on graphene and the influence of those phenomena on the electronic state of graphene. In this project, we have developed temperature-programmed terahertz (THz) emission microscopy that can map the dynamics of absorption and desorption of absorbed molecules on two-dimensional materials and determine the adsorption energy of the molecules. We obtained the first experimental value of the adsorption energy of locally physisorbed oxygen molecules on graphene and WS_2. Moreover, we have developed novel THz time domain spectroscopy (THz-TDS) with parallel-plate waveguides (PPWG) to study atomically thin materials. We demonstrate that a low carrier density graphene, which induces less than 1% absorption in conventional THz-TDS, exhibits ~30% absorption in our PPWG-based system and the signal to noise ratio is dramatically improved.

1. Introduction

The successful isolation of monolayer graphene in 2004 and its remarkable properties found subsequently have paved the way for a new research field of two-dimensional (2D) atomic layer materials [1, 2]. Many other 2D materials have since been discovered with a wide range of characteristics, from metallic to semiconducting to insulating, opening up exciting new opportunities for the development of devices based on monolayers, bilayers, and heterostructures of 2D materials [3, 4]. However, since these materials typically consist of one or a few atomic layers, their properties are extremely susceptible to perturbations from their environment. Exposure to gases, for example, has been shown to drastically affect their electrical and optical properties [5, 6], which means that in order to realize 2D-materials-based devices, it is crucial to understand the influence of gas adsorption and desorption dynamics on their properties.

Of the possible gas adsorbates/contaminants, oxygen (O_2) is one of the most important because not only it significantly alters the properties through doping, it is also the second most abundant gas in the atmosphere and is therefore highly likely to affect the performance of devices in practical applications. Though theoretical simulations proved to be useful in understanding the interaction of O_2 molecules and/or O atoms with 2D materials, conflicting results for the adsorption energies were obtained due to the inability of the approximation functionals used to properly describe the dispersion forces [7-14]. Knowing the correct value of the adsorption energy is important since it describes the strength of the interaction of the adsorbate with the 2D material, as well as the extent to which its properties are altered.

In this project we developed temperature-programmed terahertz (THz) emission microscopy (TPTEM) to probe local O_2 adsorption and desorption dynamics in graphene and tungsten disulfide (WS_2). We used the THz emission from the surface of InP coated with monolayer graphene to observe the relative concentration of O_2 adsorbates [15, 16]. In this non-contact and non-destructive method,

femtosecond infrared (IR) laser pulses are used to generate THz waves from a spot on the substrate surface. Absorption of both the incident IR and the generated THz radiation by graphene (and other 2D materials) is very small compared to the effects of adsorption of O_2 molecules on the 2D materials to the THz emission, which allows us to use THz emission as a probe in studying O_2 adsorption.

On the other hand, it is necessary to develop novel methods capable of quantitatively measuring the influence of oxygen desorption on the electronic state of 2D materials. THz – time domain spectroscopy (TDS) is an excellent tool to non-destructively and sensitively elucidate electronic properties of materials. It is particularly efficient for the characterization of materials with thickness eventually comparable or more than the operating THz wavelength (1THz = 300 μm). However, when the samples thickness is less, even far less than the wavelength, the conventional approach, where the incident beam is normal to the sample surface, is less valuable. The change in absorption of THz radiation travelling through a nanometer thick and less absorptive samples is very small. In this case, the conventional THz–TDS technique is mainly limited by the signal to noise ratio (SNR) of the experimental setup. If the change imposed by the sample is below the SNR achievable in experiment, the conventional technique is no longer reliable.

In order to overcome such problems, we have developed a novel measurement method based on THz-TDS with parallel-plate waveguide (PPWG) which is suitable for ultrathin conductive films [17]. We utilize the PPWG in which the ultrathin conductive layer is situated half-way between the two metal waveguide plates. We maintain the advantage of long interaction length between the thin film and the propagating THz wave and we compare the response for both transverse-magnetic (TM) and transverse-electric (TE) excitation of the waveguide. We develop a new formalism for extracting quantitative dielectric parameters of the thin film from our experimental measurements. We successfully characterized low carrier density graphene after the annealing process that desorbs O_2 molecules on graphene and reduces carrier density [18]. The interaction of the TE mode to the graphene layer was optimal, leading to a substantial (~30%) change in transmission even for a sheet carrier density as low as 2×10^{11} cm^{-2}. On the other hand, conventional normal-incidence transmission THz-TDS failed to detect any signal for this carrier density.

2. Probe local O_2 adsorption and desorption dynamics in graphene and tungsten disulfide with temperature-programmed THz emission microscopy (TPTEM)

2.1 Sample Preparation

Monolayer graphene samples were prepared on polished copper foils using the chemical vapor deposition (CVD) method with methane as a precursor. Thin poly(methyl methacrylate) (PMMA) film was deposited on top of graphene to act as supporting layer during the wet transfer method. Diluted ammonium persulfate solution was used to dissolve the copper foil and then washed several times in deionized water. The floating PMMA/graphene film was carefully transferred onto InP (100) substrate to produce the CVD graphene/InP sample and air-dried before removing the PMMA film using acetone. Multilayer flakes of graphene and WS_2 prepared using the liquid phase exfoliation (LPE) technique were also used in the experiments. The starting bulk materials were first annealed before dispersing in isopropyl alcohol in appropriate concentrations. Exfoliation was facilitated by applying ultrasound using a horn-tip sonicator, followed by centrifugation and decantation of the supernatant to produce the final nanosheets dispersions. 2D materials produced this way are typically few-layered nanosheets with varying laterial dimensions. The dispersions were then drop-casted onto mildly heated semi-insulating InP (100) substrate to make the LPE graphene/InP and LPE WS_2/InP samples.

2.2 Temperature-Programmed THz Emission Microscopy

The two-dimensional (2D) materials prepared by CVD (monolayer graphene) and LPE (graphene and WS_2 nanosheets) were deposited in various semiconductor substrates in preparation for THz emission experiments. The schematic diagram of the over-all set-up of the Temperature-Programmed THz Emission Microscopy (TPTEM) experiment is shown in Fig. 1. To generate THz radiation, the samples were optically excited using near-infrared pulses from a Ti:sapphire laser (MaiTai, Spectra Physics) with a duration ~100 fs and photon energy of 1.55 eV (λ = 800 nm). The diameter of the beam was adjusted by changing the relative distance between the sample and the focusing lens nearest to it. In determining the adsorption energy, the excitation beam power used was 30 mW and the beam diameter was ~1.35 mm, while in the imaging measurements, the power was 20 mW and the diameter

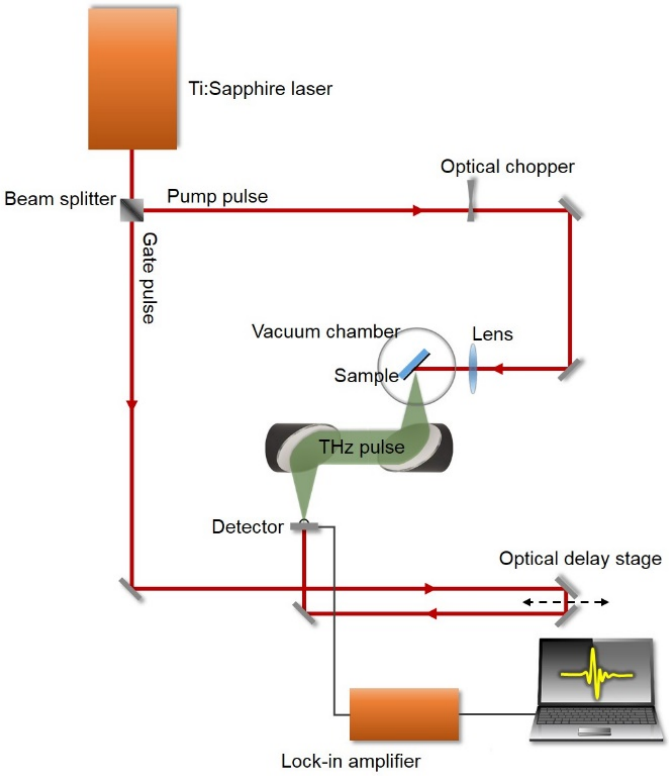

Fig. 1. Temperature-Programmed THz Emission Microscopy Set-up.

was ~0.2 mm. In all the experiments, the laser fluence was maintained at a few orders of magnitude lower than the damage threshold reported for graphene. At this range of laser fluence, THz radiation is generated mainly by ultrafast surface surge-currents in the semi-insulating InP substrates. The THz radiation emitted after optical excitation was then focused onto dipole-shaped low-temperature-grown GaAs photoconductive switch using a pair of off-axis parabolic mirrors. The output current from the switch was fed into a lock-in amplifier which was referenced to a 2.0 kHz optical chopper signal. During the measurements, the samples were placed in a vacuum chamber equipped with a PID temperature controller. The vacuum chamber containing the sample was also mounted on a computer-controlled *x-y* stage for THz imaging.

2.3 Temperature-Programmed Thermal Desorption

Traditionally, studying the kinetics of desorption in crystals is done using temperature-programmed thermal desorption (TPD). The method has also been applied in characterizing the energetics and surface stoichiometry for adsorbate on polycrystalline wires and ribbons. TPD seems to be the simplest method in obtaining a measure of the bond energy in adsorption (in comparison to calorimetric or isosteric heat measurements) since adsorption in clean metal surfaces is generally a non-activated process (which in this case, the activation energy of desorption is approximately equal to the differential heat of adsorption). Under favorable circumstances, the technique may also be used to deduce the order of reaction for desorption based on different desorption traces obtained at different initial coverages which provides a pointer to the dissociative or non-dissociative state of the adsorbate. A quantitative measure of the adsorbate present prior to thermal desorption can also be obtained using the technique in the case when the volume of the vacuum system and the pumping speed have been measured.

Fig. 2 shows the schematic diagram of the experimental set-up for temperature-programmed desorption. The crystal is first thoroughly cleaned before exposure to a controlled dosage of adsorbate gas/molecules at a given temperature. After deposition of the adsorbate layer, the crystal is heated in a controlled fashion while the partial pressure due to the desorbed species (which is approximately equal to the rate of desorption) is being recorded using, for example, a quadrupule mass analyzer. The desorption trace is then analyzed using various methods that are based on the Polanyi-Wigner equation for the rate of desorption [19],

$$-\frac{dN_{ad}}{dt} = vN_{ad}^{x}\exp\left(-\frac{E_{des}}{RT}\right) \quad (1)$$

where $-\frac{dN_{ad}}{dt}$ is the desorption rate, v is the attempt frequency, N_{ad} is the instantaneous adsorbate concentration, x is the order of desorption, E_{des} is the desorption energy (i.e., the amount of energy to break the binding energy), R is the gas constant, and R is the temperature. The most common

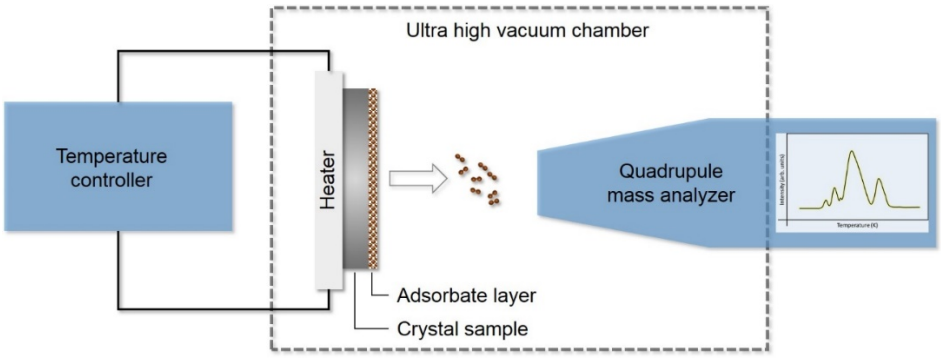

Fig. 2. Schematic diagram of experiment for temperature-programmed desorption.

method of analyzing the desorption spectrum is by plotting $\ln\left(-\frac{dN_{ad}}{dt}\right)$ versus $1/T$. If the correct order of desorption is chosen, the plot will produce a straight line and then the desorption energy can be calculated from the slope of the linear fit.

TPD is a very good technique but it also has a few major experimental pitfalls, all of which tend to broaden the desorption trace and makes the lineshape analysis unreliable.[43] One common hurdle is the temperature inhomogeneity across the adsorbent during the desorption process, which is commonly caused by the cooling effect due to the heavy support rods in the sample compartment. It is also difficult to limit the area sampled by the mass analyzer, so desorption effects occurring at the support rods and at the reaction vessel walls are also sometimes included, leading to erroneous additional peaks in the desorption spectra. The inherent large sampling area in TPD set-ups is also a big disadvantage in studying adsorption and desorption dynamics in 2D materials. Understanding local adsorption and desorption dynamics is very important because the large surface-to-volume ratio enhances the importance of surface interactions in 2D materials.

2.4 THz emission from Graphene/InP surface

The time-domain waveforms of the THz emission from graphene/InP changes with the removal of O_2 adsorbates from the graphene surface as shown in Fig. . Initially, when adsorbates are present on the graphene surface, the transient current excited by femtosecond IR pulses flows towards the surface of InP, generating a THz waveform with two peaks of opposite polarities – a dip at ~2 ps and a peak at ~2.5 ps. Significant O_2 desorption occurs upon vacuum pumping, and the change in the THz waveforms reflects the influence of the decrease in adsorbate concentration on the photoexcited current in InP. Both features in the THz waveform gradually vanish, followed by the appearance of a positive peak at ~2 ps. Irradiation with femtosecond IR pulses also promotes desorption of O_2, with the rate of desorption dependent on the laser fluence.[29] With further removal of adsorbates by annealing, the photoexcited current flows towards the bulk, and the THz emission from graphene/InP becomes similar to that of the bare InP substrate. O_2 adsorption by exposure to air reverts the THz waveform back to the initially observed waveform, and this adsorption is dramatically enhanced under UV light illumination. The change in the THz emission from graphene/InP (due to O_2 adsorption/desorption) shown in Fig. can be semi-quantitatively modeled using the relation $\vec{E}_T = x\vec{E}_1 + (1-x)\vec{E}_2$, where $\vec{E}_1$ and $\vec{E}_2$ are the initial (black) and the final (green) waveforms in Fig. , respectively, and x $(0 \geq x \geq 1)$ is their relative weight which is proportional to the concentration of adsorbed O_2 on graphene [15].

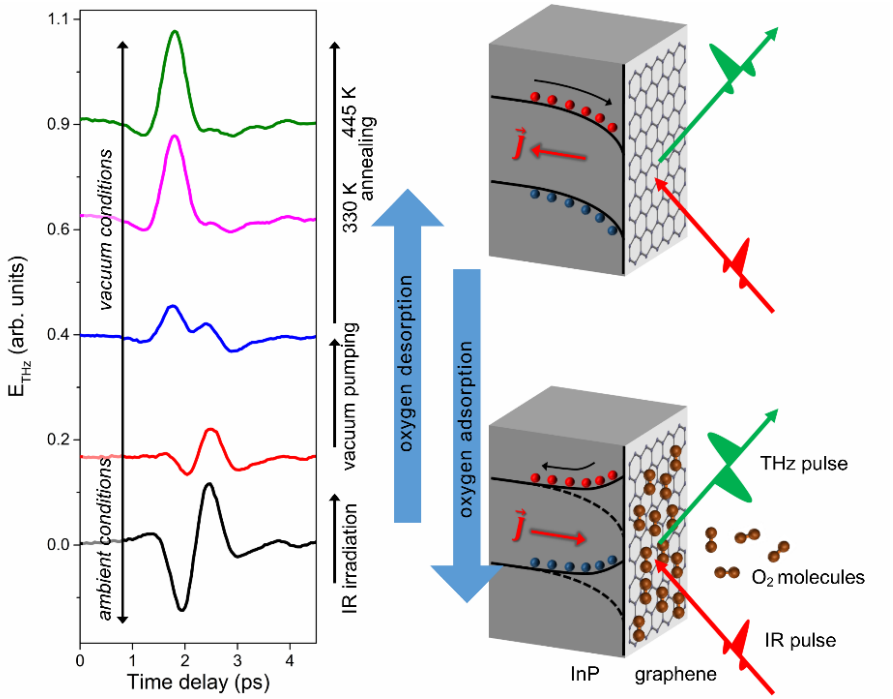

Fig. 3. THz emission waveforms from Graphene/InP measured by TPTEM.

2.5 Estimation of Adsorption Energy using TPTEM

We then used TPTEM to measure the adsorption energy of O_2 in graphene and WS_2. The experiment was designed to be similar to TDS/TPD, wherein the sample of interest is pre-exposed to a gas adsorbate and then heated in a controlled fashion while monitoring the partial pressures of the evolved molecular species by using, for example, a mass spectrometer. The main difference of TPTEM from TDS/TPD is that it can be used to monitor the relative concentration of the remaining adsorbates within the spot on the sample illuminated by the femtosecond laser. This means that it is possible to probe not only desorption dynamics but also adsorption dynamics in 2D materials within the excitation spot.

The temperature dependence of THz radiation from CVD graphene/InP before and after annealing at 445 K for 1 hour are shown in Fig. a and Fig. b, respectively (similar measurements were done for LPE graphene/InP and LPE WS_2/InP samples). By increasing the temperature of the samples, two effects take place: one is the removal of adsorbates from sample surface by thermal desorption, the other is the enhancement of the surface field in the substrate at higher temperatures.[44] Both effects lead to a relative enhancement (more positive) in the THz emission from substrate, and the first as shown here and in our previous results [15] while the latter has been observed for semi-insulating GaAs. This explains the difference in the temperature dependence of THz emission from unannealed and annealed samples. In unannealed samples, THz emission increases due to both effects, while in the annealed samples the increase in THz emission is due only to the enhancement of the surface field.

The amount of O_2 adsorbates on the surface decreases with increasing temperature, and we can separate its effect on the measured THz waveforms by simply subtracting the THz emission of annealed samples from the unannealed samples, or $E_{\text{unannealed}} - E_{\text{annealed}} \cong E_{O_2}$. The samples were annealed at 445 K for 1 hour in vacuum to make sure that the E_{annealed} waveforms represent emission from samples without adsorbates. Annealing at this temperature under vacuum conditions should completely remove physically adsorbed O_2 molecules from the surface of monolayer graphene based on optical conductivity measurements. Fig. c shows the resulting waveforms for CVD graphene/InP (similar waveforms have also been obtained for LPE graphene/InP and LPE WS_2/InP samples), while in

Fig. a we plot the change in peak values for all samples, showing decrease in absolute value with increasing temperature. The adsorbates were completely removed for CVD graphene around 413 K. However, for LPE graphene, longer annealing at 445 K was needed for further desorption, implying

that there are more strongly bonded adsorbates in LPE graphene. For LPE WS_2, the absolute peak value reaching zero at 413 K could mean either (a) complete O_2 desorption at this temperature, or (b) no further desorption happened during the annealing from 413 K to 445 K. Considering the relatively larger adsorption energy in WS_2 and the high possibility of the existence of chemisorbed species,[22,21] the latter is more likely the case.

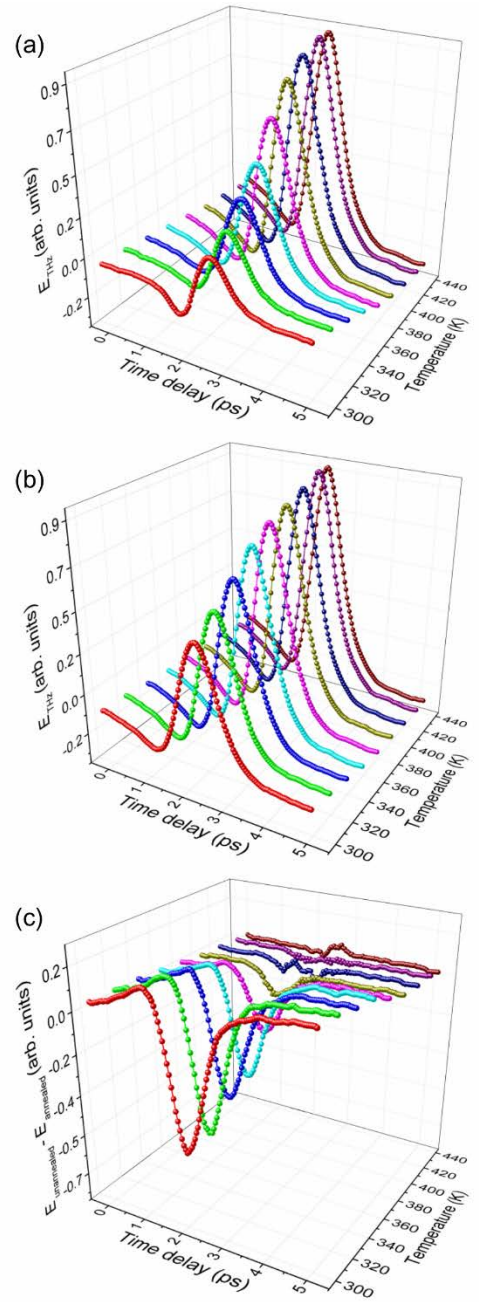

Fig. 4. THz emission from CVD Graphene/InP at different temperatures in vacuum (1×10^{-2} Pa). (a) pre-exposed in air, and (b) after annealing at 445 K for 1 hour in vacuum. (c) $E_{\text{unannealed}} - E_{\text{annealed}} \cong E_{O_2}$ at different temperatures for CVD graphene/InP.

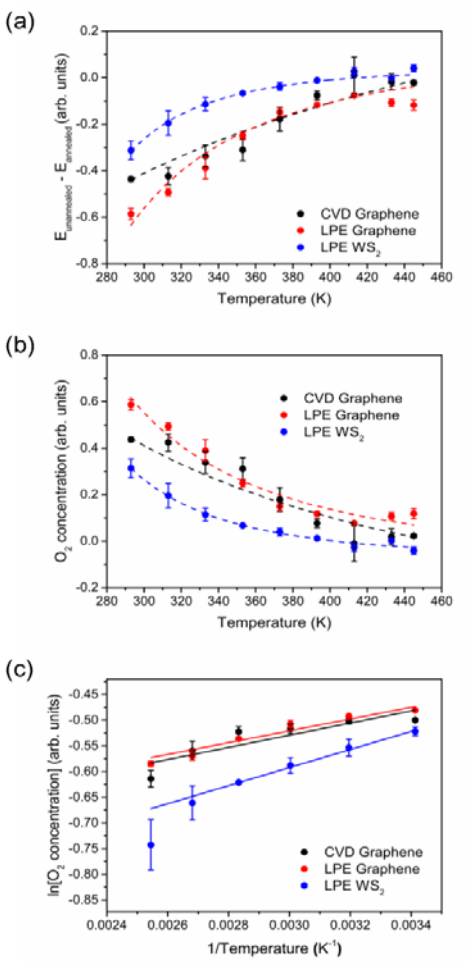

Fig. 5. Determination of the desorption energy. (a) Peak versus temperature of waveforms ($E_{\text{unannealed}} - E_{\text{annealed}} \cong E_{O_2}$) for all samples. (b) Concentration (N_{ad}) of O_2 adsorbates on surface of samples as a function of temperature. (c) $\ln(N_{ad})$ versus $1/T$ with linear fit for calculating desorption energy.

THz emission from InP primarily occurs through the surge current effect. In the far-field approximation, the amplitude of this radiation is proportional to the time derivative of the surge current, given by,

$$E_{THz} \propto \frac{\partial J(t)}{\partial t}. \tag{2}$$

The surge current, $J(t)$, is due to the transient photocarriers generated by IR excitation. One of the simplest approximations of this surge current (density) is given by the expression,

$$J(t) = q\mu(t)n(t)E_d(t), \tag{3}$$

where q is the electron/hole charge, $\mu(t)$ is the electron/hole mobility, $n(t)$ is the carrier density, and $E_d(t)$ is the driving electric field, which in this case is the built-in surface field in InP. The parameters $\mu(t)$, $n(t)$, and $E_d(t)$ determine the observed THz field through eq. (2).

Our experimental configuration as well as the observed results lead us to believe that during the O_2 adsorption/desorption process, the change in the THz radiation from graphene/InP is mainly due to the change in $E_d(t)$, which in turn is caused by the electric field on the surface of InP due to the dipoles induced by the O_2 adsorbates in graphene (E_{dipole}). Simulations show that charge transfer occurs between the O_2 molecules and carbon atoms in graphene [10], and similarly for other 2D materials [13], supporting the possibility of the existence of these electric dipoles. If we denote the modified driving field due to the presence of adsorbates as $E_{d,2} = E_{d,1} + E_{dipole}$, then the change in the THz emission from graphene/InP due to O_2 adsorbates can be obtained using eq. (2) and eq. (3) as,

$$E_{THz,2} - E_{THz,1} \propto \frac{\partial J_2}{\partial t} - \frac{\partial J_1}{\partial t} \propto E_{d,2} - E_{d,1} = E_{dipole}, \tag{4}$$

where the subscripts 2 and 1 represent the state with (unannealed) and without (annealed at 445 K) adsorbed O_2, respectively. E_{dipole} is directly proportional to the amount of charge comprising the dipole, which means that the peak of the waveforms plotted in

Fig. a is directly proportional to the concentration of the O_2 adsorbates on the surface.

The adsorbate concentration is plotted as a function of temperature in

Fig. b for all samples. From these data, we can then determine the activation energy of desorption (amount of energy needed to remove the adsorbate from the surface) through the Polanyi-Wigner equation (PWE)

$$-\frac{dN_{ad}}{dt} = vN_{ad}^{x}\exp\left(-\frac{E_{des}}{RT}\right), \quad (1)$$

where $-\frac{dN_{ad}}{dt}$ is the desorption rate, v is the attempt frequency, N_{ad} is the instantaneous adsorbate concentration, x is the order of desorption, E_{des} is the activation energy of desorption, R is the gas constant, and T is the temperature. Solving eq. (1) for N_{ad}^{x} and taking the natural logarithm of both sides, we obtain

$$\ln(N_{ad}^{x}) = \ln\left(\frac{-{}^{dN_{ad}}/_{dt}}{v}\right) + \frac{E_{des}}{R}\left(\frac{1}{T}\right), \quad (5)$$

which is a linear relationship between of $\ln(N_{ad}^{x})$ and versus ${}^{1}/_{T}$ with a slope of ${}^{E_{des}}/_{R}$.

Plots of $\ln(N_{ad}^{x})$ versus ${}^{1}/_{T}$ (with x = 1) with a linear fit for each sample are shown in

Fig. c. We assumed a first-order (x = 1) or non-dissociative desorption in our data analyses since a large energy barrier would have to be overcome for O_2 molecules to dissociate into O atoms once adsorbed in graphene and MoS_2 (a similar material to WS_2) [10]. In this case, the activation energy of desorption obtained is approximately equal to the adsorption energy. We then calculated E_{des} from the slope of the linear fits in

Fig. c, and these values are tabulated in Table 1, together with values found in the literature for comparison (values were converted to eV for easier comparison). The adsorption energies obtained using TPTEM are similar to reported theoretical values of the adsorption energy for physisorbed O_2 molecules on WS_2 and on graphene and HOPG. The chemistry and morphology of the supporting substrate significantly influence molecular interaction in graphene and possibly in other 2D materials as well. This influence becomes weaker with increasing number of layers. In our work, similar adsorption energy values were obtained for CVD monolayer graphene and LPE graphene multilayer (typically 3-4 layers) nanosheets. This leads us to believe that these values are good approximation of the actual adsorption energy of oxygen molecules on pristine graphene.

Table 1. Measured adsorption energy for physisorbed O_2 on graphene and tungsten disulfide using temperature-programmed THz emission microscope.

Sample	Adsorption energy (eV)	
	This experiment (TPTEM)	Calculations
Graphene	0.16*, 0.15**	0.13[a], 0.15[b], 0.04[c], 0.1[d], 0.01[e]
Tungsten disulfide	0.25**	0.213[f]

*Chemical vapor deposition-grown sample.

**Liquid phase exfoliated sample.

[a] O_2 molecule physisorbed on undoped graphene, obtained by first-principles calculations [10].

[b] O_2 molecule physisorbed on pristine graphene, obtained by first-principles calculations [11].

[c] O_2 molecule physisorbed on single layer graphite, obtained by density-functional calculations [8].

[d, e] O_2 molecule physisorbed on graphene, obtained by spin-unrestricted density-functional calculations [9].

[f] O_2 molecule physisorbed on WS_2 monolayer (on the most favorable site of adsorption), obtained by first-principles calculations [13].

Only the physisorbed O_2 molecules were removed in the temperature range considered in measuring E_{des}. However, it is clear that for LPE graphene a significant number of adsorbates remain at T > 400 K, which represent the O_2 molecules (or O atoms) attached to graphene at higher adsorption energies. The inherent defect sites in LPE graphene could lead to spontaneous

chemisorption of oxygen, and increasing the temperature range in this experiment should allow us to probe the desorption dynamics of these chemisorbed species.

2.6 Spatial Distribution of O_2 Molecules in Monolayer Graphene

The adsorption energies presented in Table 1 are basically averaged over the probed surface area, which is roughly the area illuminated by the femtosecond excitation pulses (with a diameter of approximately 1.35 mm). This area is still quite large in the context of 2D materials. To better understand the O_2 adsorption/desorption dynamics at different sites in the sample surface, we adjusted

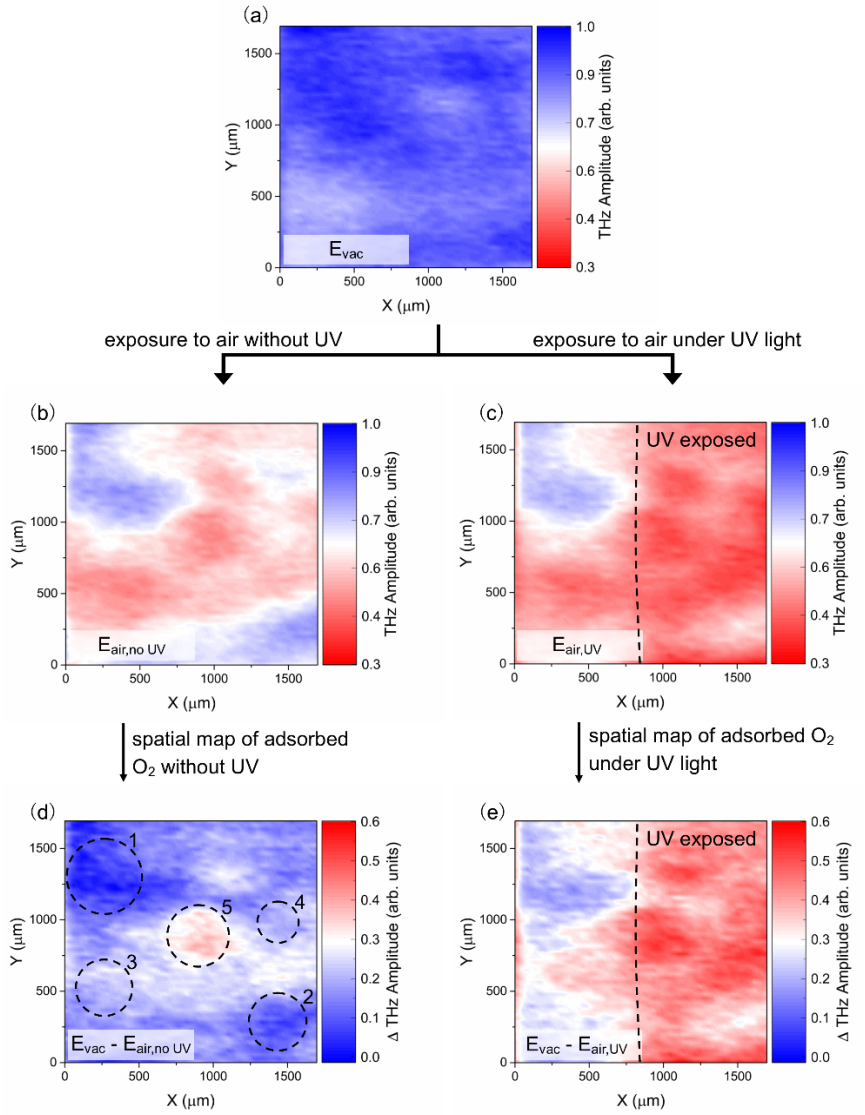

Fig. 6. THz amplitude mapping during the O_2 adsorption process. (a) THz amplitude mapping for CVD graphene/InP after annealing at 445 K in vacuum. THz mapping of the same area in sample after exposure to air for a few minutes (b) without and (c) with UV illumination. The difference in THz mapping images before and after exposure to air gives a visualization of adsorbed O_2 molecules in the graphene surface. (d) Spatial map of adsorbed O_2 molecules in graphene after exposure to air without UV illumination which reveals regions with different "natural" affinities to O_2 molecules. Regions 1 and 2 (5) show the least (highest) amount of adsorbates after exposure to air, whereas regions 3 and 4 are areas with a fair amount of adsorbates. (e) Spatial map of adsorbed O_2 molecules after exposure to air under UV illumination, showing significantly higher concentration of O_2 adsorbates in the UV exposed part. In the THz amplitude maps (a-c), the blue (red) end of the scale signifies less (more) O_2 molecules on the graphene surface, while in the ΔTHz amplitude maps (d and e), the blue (red) end of the scale signifies less (more) O_2 molecules adsorbed/added on graphene during exposure to air.

the excitation spot size to ~0.2 mm and used the imaging capability of TPTEM to study the spatial distribution of adsorbed O_2 molecules in CVD graphene at various controlled conditions. This can be done by placing the sample chamber on a computer-controlled stage.

The non-uniformity of the surface and its influence on adsorption/desorption dynamics can be clearly seen by taking THz emission images under controlled conditions. First, we removed the adsorbates in the sample by annealing it at 445 K in vacuum for at least 5 minutes, and then we monitored the spatial distribution of the relative amount of adsorbed O_2 molecules after exposure to air for a few minutes (the change in the emitted THz waveforms were similar as shown in Fig. 3). Figure 6a shows the THz amplitude map taken after removal of adsorbates from the sample surface. We then mapped the change in the THz amplitude of the same area after exposing the sample in air for a few minutes without (Fig. 6b) and with (Fig. 6c) UV illumination, which has been shown to enhance the adsorption of O_2 in graphene. The difference between the THz images before (vacuum condition) and after air exposure is taken as the measure of the adsorbed O_2 molecules. Figure 6d is the spatial distribution of O_2 adsorbates after exposure to air, which shows the "natural" affinity to O_2 molecules, *i.e.*, O_2 adsorption process without external influence like UV light, of different regions in the sample surface. Regions 1 and 2 (5) in Fig. 6d show the least (highest) amount of adsorbates after exposure to air, whereas regions 3 and 4 are areas with a fair amount of adsorbates. Illumination with UV during exposure to air promotes more O_2 adsorption, and this dramatic effect can be seen in Fig. 6e, where UV light was selectively focused on the graphene surface during exposure to air. The image clearly shows a higher concentration of adsorbates in the area exposed to UV.

The results presented here reveal the possibility of using our technique in performing quantitative and imaging studies in the O_2 adsorption and desorption in 2D materials in a non-destructive way. Since the primary requirement for this technique to work is that the gas adsorbates should induce local electric dipoles that will change the THz emission from InP, TPTEM is expected to be useful for studying the adsorption and desorption dynamics of other types of gas molecules in any 2D material, such as NH_3, as long as charge transfer occurs between the adsorbate and the 2D material in question. All these results promise the possibility of doing local spatiotemporal studies on the molecular adsorption and desorption on a variety of 2D materials. It is also possible to combine TPTEM with other techniques such as Raman microscopy to study the dependence of gas adsorption on the structural properties of the 2D material, and photoluminescence microscopy to determine the effect of gas adsorption to its optical properties.

3. Evaluation of low carrier density graphene with parallel plate waveguide THz time domain spectroscopy (PPWG-THz-TDS)

3.1 Experimental setup

Figure 7 shows schematic of THz-PPWG-TDS. The PPWG is made of two blocks of aluminum with same dimensions. The width, length and thickness of the waveguide are 30 mm, 10 mm and 15 mm respectively. The inside face of waveguide is hand polished with 320 grit sandpapers. Then, the aluminum surfaces are coated with tens nanometer of titanium and subsequently coated with gold of

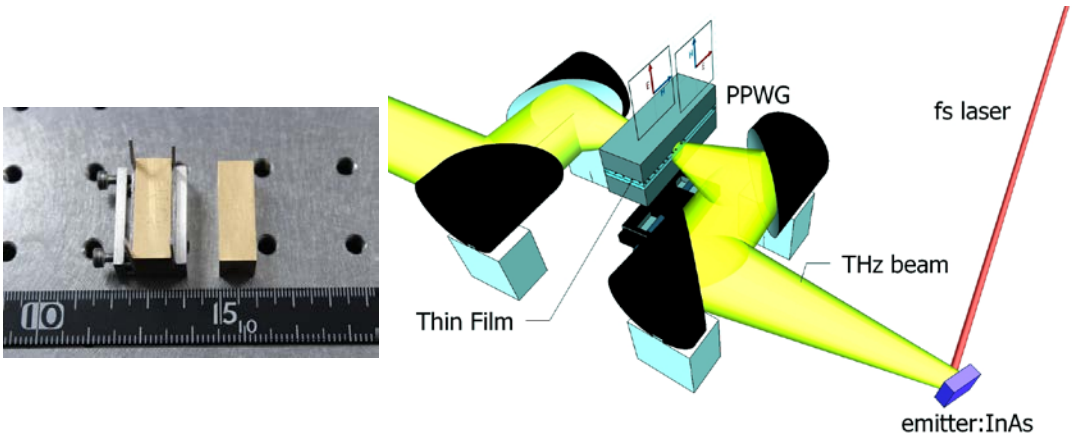

Figure 7 Schematic of the main part of THz-PPWG-TDS. The description is in the main text.

about 200 nm thickness. The coating plays two roles: to avoid roughness and to increase the conductivity of plates.

In this work, substrates are used to simultaneously fill the space between the plates of PPWG and to support the thin conductive films. Then, the thickness of the substrates determines the plate separation. Actually, two substrates of 0.5 mm thickness, 30 mm width and 10 mm length are employed. The ultrathin conductive films are always deposited onto half width (15 mm) of one of the substrate surface. This substrate with half side coated by the samples is first set on the top of the bottom waveguide. Another bare substrate is next placed on top of the half coated substrate. Finally, we put the top plates of the waveguide. A small sample holder is fabricated to align substrates to the waveguide plates. The whole waveguide system is mounted on mechanical stage and placed at the center of the second parabolic and third parabolic mirror. The mechanical stage can be automatically handled outside the THz-PPWG-TDS system.

Since half of the waveguide contains conductive film located between the plate and half-filled solely with substrate, we can set the reference signal and the sample signal. The reference signals are the THz pulses transmitted through PPWG with substrate. The sample signals are the THz pulses transmitted through PPWG with thin films on substrate. The setting we have just described above greatly facilitates the recording of the reference and the sample signals. We first record a number of THz pulses from the reference side. After that, the waveguide is moved perpendicularly with respect to the beam propagation direction. Then, a number of THz pulses are recorded from the sample side.

A mode-locked femtosecond laser Mai tai (Spectra Physics, Ti: sapphire laser) delivers a near infrared optical pulses at a wavelength of 800 nm and a repetition rate of 80MHz. The pulse width of the laser is less than 80 fs with a maximum power of 2W. The laser with a power about 90mW is focused on the surface of holes doped (p-type) indium arsenide (InAs) wafer to generate THz wafes. It is well known that in this situation, the main relevant mechanism for THz generation in narrow-band gap semiconductors is the photo-Dember effect. The detection of THz radiation is realized by low-temperature grown gallium arsenide (LT-GaAs) photoconductive antenna (PCA).

The emitted THz is collimated, polarized and focused onto the input face of the PPWG. After traveling through the waveguide, this output THz beam is collimated, polarized and focused to the detector. The detected current is amplified and sent to a lock-in amplifier which is phase locked to the chopper frequency for the synchronous detection. The electronic detection system and the delay stage controller is synchronized by a LabVIEW computer program. The mechanical stage for waveguide is manually controlled. The THz-PPWG-TDS system is encased inside an acrylic box and purged with nitrogen to minimize the noise due to the water vapor absorption.

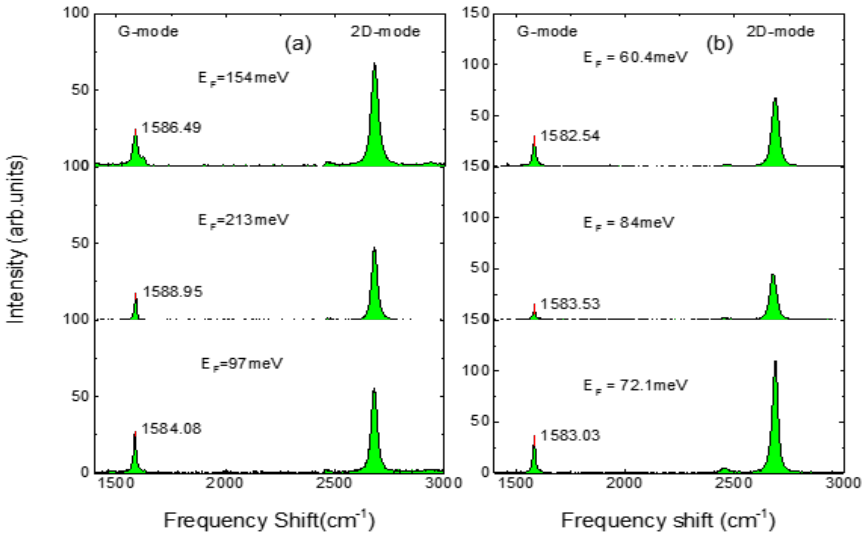

Figure 8 Raman Spectra of graphene sample and the Fermi energy associated. Each Raman spectrum is measured in one spot of the substrate side with graphene. The frequency positions of G-mode peaks are also shown. The difference in intensities is due to the difference of the laser pump power used in Raman spectroscopy. The unit of the frequency shift of the figures is cm^{-1}. (a). Raman spectra of sample A before annealing. (b). Raman spectra of sample A after annealing.

The samples used in this study were provided by Ajayan's group of Rice University. Two graphene samples (Samples A and B) are grown using chemical vapor deposition (CVD). A copper foil was placed in the deposition chamber and annealed at a temperature of 1000°C in a hydrogen/argon gas at a pressure of 1 Torr for 20 min. Methane was introduced into the chamber with a flow rate of 4 standard cubic centimeters per minute (sccm) for 10 min. The sample was cooled for 20 min in a hydrogen/argon gas. The grown graphene layer was then transferred onto two MgO (100) substrates, which were transparent in the THz frequency range. The dimensions of the MgO substrate were also 30 mm (width) × 10 mm (length) × 0.5 mm (thickness). Half of the substrate was covered by CVD graphene.

Raman spectroscopy characterization, as shown in Fig.8, provides an insight of graphene properties in versatile way and nondestructive fashion. Raman measurements allow, amongst other, ascertaining the quality of the samples (quality of growth and transfer in our case). Here, we only focus on the basic operation and measurements in Raman spectroscopy. In brief, the so-called G–mode spectrum and 2D-mode spectrum are used to characterize graphene (single or multi layers) in Raman spectroscopy. G–mode is 2D–mode originate from in-plane vibrational mode of graphene. The peak intensity ratio I_{2D}/I_G indicates the layer number of graphene. A single layer graphene yields at least a ratio more than 1.5. Here, Raman spectroscopy Xplora One was used to probe the sample at different spots. The intensity ratio of the G mode to the 2D mode in Raman spectra in Fig.8 confirms that monolayer graphene was grown.

3.2 Comparison between conventional THz-TDS and THz – PPWG – TDS:

The measurements procedures in THz-PPWG-TDS has been already described previously. Here we use the second experimental setup which has a different parabolic mirror focal length. Characterization measurements of each graphene sample were performed in two steps. First, we characterize the samples using PPWG and conventional THz-TDS systems. Then, we annealed the sample at 445 K under a pressure of ~10^{-7} Torr in a cryostat for one hour followed by cooling for about four hours in the vacuum chamber, after which we immediately measured the sample again with both systems. The purpose of sample annealing is to obtain a pristine graphene which is free of impurities.

Before embarking in detailed discussion, we first compare spectra taken by conventional transmission THz- TDS with those taken in TE mode of THz-PPWG-TDS in Fig. 9. The sample characterized in this Fig. is the graphene after annealing (almost pure graphene). The comparison of both spectrum already indicates that it is challenging to measure the optical properties of pristine graphene in conventional method. The spectrum of the reference MgO and graphene/MgO almost overlap over the entire range of frequency. In contrast, an obvious amplitude difference occurs in TE mode of PPWG spectrum.

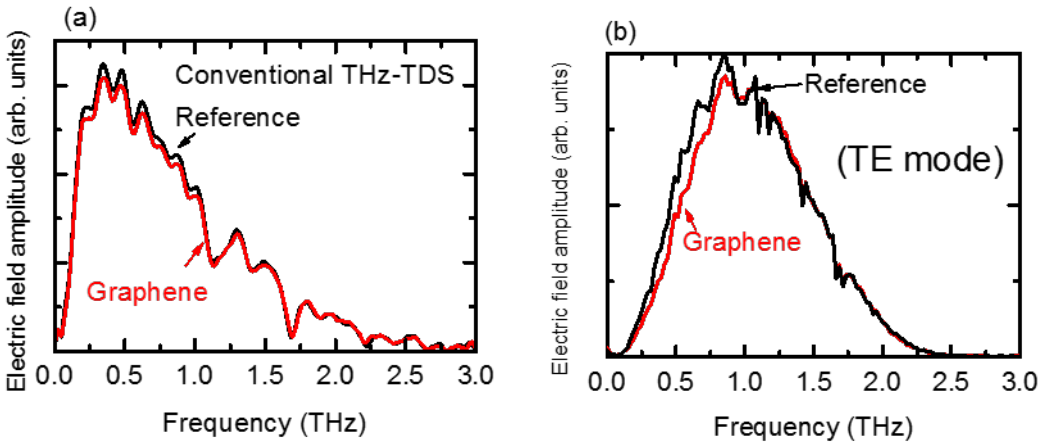

Figure 9 Comparison of spectra measured using (a) conventional THz- TDS and (b) by THz-PPWG-TDS in TE mode.

To further confirm the advantage of PPWG, Fig. 10 shows the transmittance spectra for Sample A taken by means of both methods. In the case of conventional THz-TDS, the spectra are nearly flat over the entire frequency range (0.1 THz-1.8 THz) for the sample before and after annealing, with transmittance ~95% and ~98%, respectively. It should be noted that each transmission data collected using conventional THz-TDS was averaged over 20 spectra. In the case of -THz-PPWG-TDS, the transmittance clearly shows some frequency dependence. The transmittance value is ~60% (~70%) before (after) annealing in the low-frequency region while it increases to ~95% at the high-frequency end of the spectra.

The spectrum of TE–mode of PPWG (Fig. 10) suggests from the absence of interferences that single-mode propagation is realized. Then, in the frequency (*f*) domain, the complex-valued transmission coefficient is simplified to:

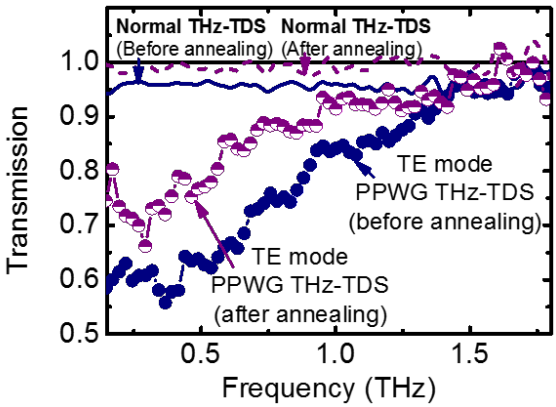

Figure 10 Comparison of frequency dependent transmission data taken with normal-incidence transmission THz-TDS and THz- PPWG-TDS in TE mode. (Sample A before and after annealing). The upper quasi-flat curves are averaged transmittance data taken with THz-TDS. The blue solid curve is for non-annealed graphene on MgO and the purple dashed curve is for annealed graphene on MgO. The same sample is analyzed with TE waveguide mode, leading to a frequency-dependent transmittance represented by blue solid circles for Sample A before annealing and by purple solid circles for after annealing.

$$T(f) = \frac{E_{MgO/Graphene/MgO}}{E_{MgO/MgO}} = |T| e^{i\Delta\varphi} \qquad (6)$$

where $E_{\mathrm{MgO/Gr/MgO}}$ is the complex frequency-dependent electric field detected through the waveguide with graphene, $E_{\mathrm{MgO/MgO}}$ is the electric field detected through the waveguide without graphene, $\Delta\varphi$ is the experimental phase difference between the reference and the sample pulses, $\gamma \equiv \Delta\beta - j\Delta\alpha$, β is the propagation constant of the PPWG mode under consideration (TE or TM mode), and α is the propagation loss. The length of the waveguide, *L*, is 10 mm. In Eq. (6), the coupling coefficient and the impedance matching are assumed to be the same for the reference and sample signal. Note that Eq. (6) works only for single-mode propagation, either in the TE mode or TM mode.

3.3 Conductivity results

Figure 11 shows the real and imaginary parts of the sheet conductivity for Sample A and B before and after annealing, together with fitting curves using the Drude formula. The conductivity is expressed in units of σ_0, where $\sigma_0 = \pi e^2/2h \approx 6.1 \times 10^{-5}$ S is the universal interband conductivity of graphene. From the relation between E_F and the carrier concentration *N*, we found that $N = 1.07 \times 10^{12}$ cm^{-2} for Sample A and $N = 1.01 \times 10^{12}$ cm^{-2} for Sample B before annealing. The scattering rate obtained were $\Gamma = 3.39\ 10^{12}$ s^{-1} for Sample A and $\Gamma = 4.2\ 10^{12}$ s^{-1} for Sample B. These values are comparable with the values reported for CVD-grown graphene on different substrates [20, 21].

Table 2 shows the fitting parameters of the Drude model extracted from the experimental data for both Sample A and Sample B: the DC conductivity(S), scattering rate, Γ (s^{-1}), carrier density, *N* (cm^{-2}), Fermi Energy, E_F (meV) and the mobility ($\mathrm{cm}^{-2}\mathrm{V}^{-1}\mathrm{s}^{-1}$). It has been experimentally observed that adsorption of water and oxygen molecules dramatically changes the electromagnetic properties of graphene. In fact, transport measurements in previous works revealed that charge transfer occurs between adsorbed molecules and graphene [22]. Vacuum annealing described in the experimental section removes these adsorbed molecules and additionally reduces PMMA residues and other

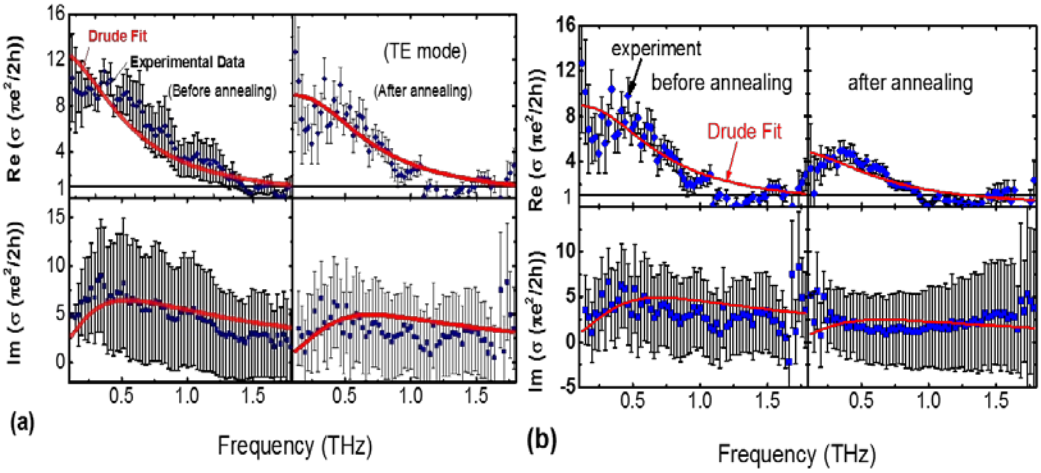

Figure 11. Experimental data of graphene conductivity and the Drude model fitting curves normalized by the universal conductivity of graphene ($\pi e^2/2h$). (a) Results for Sample A and (b) results for Sample B. The error bars indicate the standard deviation of the experimental data. The red curve is the theoretical Drude fit while the frequency range used for the fitting process was set to be 0.1-1.8 THz

impurities. It can indeed be seen in Table 2 that the annealing process reduces the carrier density (N = 2.3×10^{11} cm^{-2} for Sample A and $N = 2.2 \times 10^{11}$ cm^{-2} for Sample B). These small numbers of densities were determined by the THz-PPWG-TDS method while normal THz-TDS could not detect any THz absorption after annealing, as also shown Table 1 for Sample A.

.

Table 2 The fitting parameters of the Drude model extracted from the experimental data for both Sample A and Sample B: the DC conductivity(S), scattering rate, Γ (s^{-1}), carrier density, N (cm^{-2}), Fermi Energy, E_F (meV) and the mobility (cm-^{2}V^{-1}s^{-1}).

	Sample A			Sample B	
	Before annealing		After annealing	Before annealing	After annealing
	PPWG	THz-TDS	PPWG	PPWG	PPWG
σ_0 (mS)	78	86.5	36.7	71	36.2
Γ(10^{12} s^{-1})	3.39	5.84	2.6	4.2	4.08
N (10^{12} cm^{-2})	1.07	1.94	0.23	1.01	0.22
E_F (meV)	133	179	62.1	129	61
μ(cm-^{2}V^{-1}s^{-1})	3750	1972	8105	4393	10200

References

[1] Novoselov, K. S.; Geim, A. K.; Morozov, S. V; Jiang, D.; Zhang, Y.; Dubonos, S. V; Grigorieva, I. V; Firsov, A. A. Electric Field Effect in Atomically Thin Carbon Films. Science 2004, 306, 666–669.

[2] Geim, A. K.; Novoselov, K. S. The Rise of Graphene. Nat. Mater. 2007, 6, 183–191.

[3] Xia, F.; Wang, H.; Xiao, D.; Dubey, M.; Ramasubramaniam, A. Two-Dimensional Material Nanophotonics. Nat. Photonics 2014, 8, 899–907.

[4] Yazyev, O. V.; Chen, Y. P. Polycrystalline Graphene and Other Two-Dimensional Materials. Nat. Nanotechnol. 2014, 9, 755–767.

[5] Schedin, F.; Geim, A. K.; Morozov, S. V.; Hill, E. W.; Blake, P.; Katsnelson, M. I.; Novoselov, K. S. Detection of Individual Gas Molecules Adsorbed on Graphene. Nat. Mater. 2007, 6, 652–655.

[6] Docherty, C. J.; Lin, C.-T.; Joyce, H. J.; Nicholas, R. J.; Herz, L. M.; Li, L.-J.; Johnston, M. B. Extreme Sensitivity of Graphene Photoconductivity to Environmental Gases. Nat. Commun. 2012, 3, 1228.
[7] Lamoen, D.; Persson, B. N. J. Adsorption of Potassium and Oxygen on Graphite: A Theoretical Study. J. Chem. Phys. 1998, 108, 3332.
[8] Sorescu, D. C.; Jordan, K. D.; Avouris, P. Theoretical Study of Oxygen Adsorption on Graphite and the (8,0) Single-Walled Carbon Nanotube. J. Phys. Chem. B 2001, 105, 11227–11232.
[9] Giannozzi, P.; Car, R.; Scoles, G. Oxygen Adsorption on Graphite and Nanotubes. J. Chem. Phys. 2003, 118, 1003.
[10] Yan, H. J.; Xu, B.; Shi, S. Q.; Ouyang, C. Y. First-Principles Study of the Oxygen Adsorption and Dissociation on Graphene and Nitrogen Doped Graphene for Li-Air Batteries. J. Appl. Phys. 2012, 112, 104316.
[11] Guang, H.; Aoki, M.; Tanaka, S.; Kohyama, M. First-Principles Prediction on Adsorption of Oxygen Molecule onto Defect in Single-Layer Graphene. Trans. Mater. Res. Soc. Japan 2013, 38, 477–480.
[12] Liu, H.; Han, N.; Zhao, J. Atomistic Insight into the Oxidation of Monolayer Transition Metal Dichalcogenides: From Structures to Electronic Properties. RSC Adv. 2015, 5, 17572–17581.
[13] Zhou, C.; Yang, W.; Zhu, H. Mechanism of Charge Transfer and Its Impacts on Fermi-Level Pinning for Gas Molecules Adsorbed on Monolayer WS2. J. Chem. Phys. 2015, 142, 214704.
[14] Mehmood, F.; Pachter, R.; Lu, W.; Boeckl, J. J. Adsorption and Diffusion of Oxygen on Single-Layer Graphene with Topological Defects. J. Phys. Chem. C 2013, 117, 10366–10374.
[15] Sano, Y.; Kawayama, I.; Tabata, M.; Salek, K. A.; Murakami, H.; Wang, M.; Vajtai, R.; Ajayan, P. M.; Kono, J.; Tonouchi, M. Imaging Molecular Adsorption and Desorption Dynamics on Graphene Using Terahertz Emission Spectroscopy. Sci. Rep. 2014, 4, 6046.
[16] Bagsican, F. R.; Zhang, X.; Ma, L.; Wang, M.; Murakami, H.; Vajtai, R.; Ajayan, P. M.; Kono, J.; Tonouchi, M.; Kawayama, I. Effect of Oxygen Adsorbates on Terahertz Emission Properties of Various Semiconductor Surfaces Covered with Graphene. J. Infrared, Millimeter, Terahertz Waves 2016, 1–7.
[17] M. Razanoelina, R.Kinjo, K. Takayama, I. Kawayama, H. Murakami, Daniel M. Mittleman and M. Tonouchi, “Parallel-Plate Waveguide Terahertz Time Domain Spectroscopy for Ultrathin Conductive Films" Journal of Infrared, Millimeter, and Terahertz Waves, Vol. 36, Issue 12, pp 1182-1194 (2015)
[18] Manjakavahoaka Razanoelina, Filchito Renee Bagsican, Iwao Kawayama, Xiang Zhang, Lulu Ma, Hironaru Murakami, Robert Vajtai, Pulickel M. Ajayan, Junichiro Kono and Masayoshi Tonouchi, “Probing low-density carriers in a single atomic layer using terahertz parallel-plate waveguides" Optics Express Vol. 24, pp. 3885-3893 (2016)
[19] Redhead, P. A. Thermal Desorption of Gases. Vacuum 1962, 12, 203–211.
[20] J. Horng, C.-F. Chen, B. Geng, C. Girit, Y. Zhang, Z. Hao, H. A. Bechtel, M. Martin, A. Zettl, M. F. Crommie, Y. Ron Shen, and Feng Wang, “Drude conductivity of Dirac fermions in graphene,” Phys. Rev. B 83, 165113 (2011).
[21] L. Ren, Q. Zhang, J. Yao, Z. Sun, R. Kaneko, Z. Yan, S. Nanot, Z. Jin, I. Kawayama, M. Tonouchi, J. M. Tour, and J. Kono, “Terahertz and Infrared Spectroscopy of Gated Large-Area Graphene,” Nano Lett. 12(7), 3711-3715 (2012).
[22] F. Schedin, A. K. Geim, S. V. Morozov, E. W. Hill, P. Blake, M. I. Katsnelson, and K. S. Novoselov, “Detection of individual gas molecules adsorbed on graphene,” Nat. Mater. 6, 652-655 (2007).

List of Publications and Significant Collaborations that resulted from your AOARD supported project:

a) Papers published in peer-reviewed journals,

1) Bagsican, F. R.; Winchester, A.; Ghosh, S.; Zhang, X.; Ma, L.; Wang, M.; Murakami, H.; Talapatra, S.; Vajtai, R.; Ajayan, P.; Kono, J.; Tonouchi, M.; Kawayama, I. Adsorption energy of oxygen molecules on graphene and two-dimensional tungsten disulphide. *Scientific Reports* 2017, 7, 1774.

2) Bagsican, F. R.; Zhang, X.; Ma, L.; Wang, M.; Murakami, H.; Vajtai, R.; Ajayan, P.; Kono, J.;

Tonouchi, M.; Kawayama, I. Effect of Oxygen Adsorbates on Terahertz Emission Properties of Various Semiconductor Surfaces Covered with Graphene. *J. Infrared Milli. Terahz. Waves* 2016, 37, 1117–1123.

3) Bagsican, F. R.; Kawayama, I.; Murakami, H.; Tonouchi, M.; Winchester, A.; Ghosh, S.; Talapatra, S. Laser THz Emission Spectroscopy of Gas Adsorption-Desorption Dynamics in Tungsten Disulfide Nanosheets. *Surf. Sci. Nanotech* 2016, *14*, 78–82.

4) Razanoelina M., Bagsican F., Kawayama. I., Zhang, I., Ma, L., Murakami, H., Vajitai, R., Ajayan, P. M., Kono, J., Tonouchi, M., "Probing low-density carriers in a single atomic layer using terahertz parallel-plate waveguides," Opt. Express **24** (4), 3885-3893 (2016).

b) Papers published in peer-reviewed conference proceedings,

1) Bagsican, F. R.; Gonzales, J.; Zhang, X.; Ma, L.; Kawayama, I.; Murakami, H.; Vajtai, R.; Ajayan, P.; Kono, J.; Tonouchi, M. Laser Terahertz Emission Spectroscopy of Graphene/InAs Junctions. *MRS Proc.* 2015, *1808*, 1-7.

2) Razanoelina M., Bagsican F., Kawayama. I., Zhang, I., Ma, L., Murakami, H., Vajitai, R., Ajayan, P. M., Kono, J., Mittleman, D. M and M. Tonouchi, "Parallel plate waveguide time domain spectroscopy to study terahertz conductivity of utltrathin materials", Advanced Applications in Industry and Defense, Vol. Proc. SPIE 9856, Pages 985605 (2016)

c) Papers published in non-peer-reviewed journals and conference proceedings

1) Iwao Kawayama, "Characteristics of Terahertz Wave Emission from Graphene/Seimiconductor Junctions", IEICE Technical Report, ED2014-113,pp. 85-89 December, 2014

d) Conference presentations without papers,

1) F.R. Bagsican, I. Kawayama, H. Murakami, A. Winchester, S. Ghosh, S. Talapatra, and M. Tonouchi, "Terahertz emission from semi-insulating InP surface coated with WS_2 nanosheets prepared by liquid phase exfoliation," The 7th International Symposium on Surface Science (3pE2-2), Matsue, Shimane, Japan, November 2-6, 2014.

2) F.R. Bagsican, I. Kawayama, H. Murakami, A. Winchester, S. Ghosh, S. Talapatra, and M. Tonouchi, "Infrared-Induced Photo-Oxidation in WS_2 Nanosheets Observed using Laser Terahertz Emission Spectroscopy," Optical Terahertz Science & Technology Conference (OTST) 2015, San Diego, USA, March 8-13, 2015.

3) (Invited) M.Tonouchi, "Laser Terahertz Emission Microscope for Material Science", MRS Spring Meeting, 2015/4/6-2015/4/10, San Francisco, USA.

4) (Invited) Iwao Kawayama, Saikat Talapatra, Robert Vajtai, Pulickel M. Ajayan, Junichiro Kono, Tonouchi Masayoshi, "Study on gas molecule adsorption-desorption dynamics on graphene using terahertz emission spectroscopy", SPIE De-fense,Security,and Sensing, 2015/4/20-2015/4/23, Baltimore Convention Center, USA

5) (Invited) I. Kawayama, "Absorption and desorption dynamics of gas molecules on 2D Nanomaterials observed by terahertz spectroscopy", Nanotechnology congress & Expo, 2015/8/11-2015/8/13, Fleming's Conference Hotel Frankfurt, Germany

6) (Invited) M.Tonouchi, "Laser Terahertz Emission Microscope for Material Science and Industrial Applications", Shenzhen Inter-national Conference on Advanced Science and Technology 2015, 2015/8/18-2015/8/22, Shenzhen, China

7) F.R. Bagsican, A. Winchester, S. Ghosh, X. Zhang, L. Ma, M. Wang, I. Kawayama, H. Murakami, R. Vajtai, P.M. Ajayan, J. Kono, S. Talapatra, and M. Tonouchi, "Gas Adsorption Dynamics in Graphene by Laser THz Emission Spectroscopy," Joint JSAP & OSA Symposium (15a-2D-7), Nagoya, Japan, September 13-16, 2015.

8) (Invited) M. Razanoelina, I. Kawayama, H. Murakami, and M. Tonouchi, "Parallel Plate Waveguide Terahertz–Time Domain Spectroscopy for Ultrathin Metallic Films ", East Asian

Symposium on Superconductive Electronics 2015, 2015/11/4-2015/11/6, Daejeon, Korea

9) (Invited) Manjakavahoaka Razanoelina, Filchito Renee Bagsican, Iwao Kawayama, Xiang Zhang, Lulu Ma, Wiley, Hironaru Murakami, Robert Vajtai, Pulickel M. Ajayan, Junichiro Kono, Daniel M. Mittleman, Masayoshi Tonouchi, “Parallel plate waveguide time domain spectroscopy to study terahertz conductivity of utltrathin materials”, SPIE; Terahertz Physics, De-vices, and Systems , 2016/4/17-2016/4/21, Baltimore Convention Center, USA

10) F.R. Bagsican, A. Winchester, S. Ghosh, X. Zhang, L. Ma, M. Wang, I. Kawayama, H. Murakami, S. Talapatra, R. Vajtai, P.M. Ajayan, J. Kono, and M. Tonouchi, “Evaluation of Local Adsorption Energy of Oxygen on Graphene using Laser THz Emission Spectroscopy,” Conference on Lasers and Electro-Optics (CLEO) 2016, San Jose, California, USA, June 5-10, 2016.

11) F. Bagsican, I. Kawayama, A. Winchester, S. Ghosh, X. Zhang, L. Ma, M. Wang, H. Murakami, S. Talapatra, R. Vajtai, P. Ajayan, J. Kono, and M. Tonouchi, “Binding Energy of Locally Physisorbed Oxygen Molecules in 2D Materials Measured by Laser Terahertz Emission Microscopy,” JSAP-OSA Joint Symposia, Niigata, Japan, September 13-16, 2016.

12) (Invited) M. Razanoelina, F. R. Bagsican, X. Zhang, L. Ma2 H. Murakami, R. Vajtai, P. M. Ajayan, J. Kono, D. Mittelman, M. Tonouchi and I. Kawayama, “Parallel Plate Waveguide Terahertz Time Domain Spectroscopy for 2D materials”, IRMMW-THz 2016 , Bella Center Copenhagen, Denmark, 29 Sep. 2016

13) F. R. Bagsican, I. Kawayama, A. Winchester, S. Ghosh, X. Zhang, L. Ma, M. Wang, H. Murakami, S. Talapatra, R. Vajtai, P. M. Ajayan, J. Kono, and M. Tonouchi, “Temperature-programmed desorption measurements of oxygen molecules in 2D materials using laser terahertz emission microscopy,” 41st International Conference on Infrared, Millimeter and Terahertz Waves (IRMMW-THz), Copenhagen, Denmark, Sept. 25-30, 2016.

14) (Invited) M.Tonouchi, "Terahertz emission study of molecular adsorption dynamics onto graphene prepared on InP substrates”, The Seventh International Symposium on Terahertz Nanoscience (TeraNano VII), October 2-8, 2016, Porquerolles, France

15) (Invited) I. Kawayama and M.Tonouchi, "Study on local oxygen absorption/desorption dynamics onto 2D materials probed by potential-sensitive THz radiation", The 8th International Symposium on Ultrafast Phenomena and Terahertz Waves (ISUPTW 2016), Oct.10-12, 2016, Chongqing, China.

16) (Invited) M. Tonouchi, “Parallel Plate Waveguide Terahertz Time Domain Spectroscopy”, 5th Russia-Japan-USA-Europe Symposium on Fundamental & app;ied Problems of Terahertz Devices & Technologies, Sakura Hall, Katahira Campus, Tohoku University, Sendai, Japan(Nov 2016)

17) M. Razanoelina, I. Kawayama, Xiang Zhang, Hironaru Murakami, Robert Vajtai, Pulickel M. Ajayan, , Junichiro Kono, D. M. Mittleman, M. Tonouchi, "Terahertz Parallel Plate Waveguide to Evaluate Electrical Transport Properties of 2D Materials" Conference on Lasers and Electro-Optics, (CLEO), 2016/12

18) F. Bagsican, A. Winchester, S. Ghosh, X. Zhang, L. Ma, M. Wang, H. Murakami, S. Talapatra, R. Vajtai, P. M. Ajayan, J. Kono, M. Tonouchi, and I. Kawayama, “Adsorption energy of physisorbed oxygen molecules on 2D materials measured by laser terahertz emission microscopy,” Optical Terahertz Science & Technology Conference (OTST) 2017, London, UK, April 2-7 2017.

19) (Invited) I. Kawayama, “Terahertz Spectroscopy of Graphene”, Collaborative Conference on Materials Research (CCMR) 2017, 2017/6/26-2017/6/30, International Convention Center (ICC) Jeju , Korea

20) (Invited) I. Kawayama, “Terahertz Time-Domain Spectroscopy of CVD Graphene in a Wide Temperature Range”, International union of materials research society-International conference of advanced materials 2017, 2017/8/27-2017/9/1, Kyoto, Japan

21) (Invited) Filchito Renee Bagsican, Andrew Winchester, Sujoy Ghosh, Xiang Zhang, Lulu Ma, Minjie Wang, Hironaru Murakami, Saikat Talapatra, Robert Vajtai, Pulickel M. Ajayan, Junichiro Kono, Masayoshi Tonouchi, and Iwao Kawayama, “Probing oxygen adsorption in 2D materials using laser terahertz emission microscopy,” Global Nanophotonics 2017, Dec. 6-8,

2017, Palawan, Philippines.

22) (Invited) Filchito Renee Bagsican, Andrew Winchester, Sujoy Ghosh, Xiang Zhang, Lulu Ma, Minjie Wang, Hironaru Murakami, Saikat Talapatra, Robert Vajtai, Pulickel M. Ajayan, Junichiro Kono, Masayoshi Tonouchi, and Iwao Kawayama, "New method to estimate oxygen adsorption energy on 2D materials with terahertz emission microscopy," The 4th Int'l. Symposium on Microwave/Terahertz Science and Applications, the 8th Int'l. Symposium on Terahertz Nanoscience, and the OptoX NANO, Nov. 19-23, 2017, Okayama Convention Center, Okayama, Japan.

23) M. Razanoelina, S. Ohashi, I. Kawayama, H. Murakami, , R. Vajtai, P. M. Ajayan, J. Kono and M. Tonouchi and, "Limitations of the parallel plate waveguide in terahertz spectroscopy of ultrathin and low conductive materials", The 8th International Symposium on Terahertz Nanoscience, Current trends in Optical and X-Ray metrologies of key enabling nanomaterials/devices for the Ubiquitous Society, renewable energy and health, Okayama Convention Center, Japan 2017/11/19-11/23

e) manuscripts submitted but not yet published
N/A

f) provide a list any interactions with industry or with Air Force Research Laboratory scientists or significant collaborations that resulted from this work.

- We have collaborated with Prof. Kono group and Prof. Ajayan group in Rice University through this project.
- We have started collaborative research on the interaction between terahertz waves and tobogical insulators, surface nanostructures and 2D materials with Dr. Augustine Urbas of the US Air Force Research Institute.

Attachments: Publications a), b)

DD882: As a separate document, please complete and sign the inventions disclosure form.

Important Note: If the work has been adequately described in refereed publications, submit an abstract as described above and refer the reader to your above List of Publications for details. If a full report needs to be written, then submission of a final report that is very similar to a full length journal article will be sufficient in most cases. This document may be as long or as short as needed to give a fair account of the work performed during the period of performance. There will be variations depending on the scope of the work. As such, there is no length or formatting constraints for the final report. Keep in mind the amount of funding you received relative to the amount of effort you put into the report. For example, do not submit a $300k report for $50k worth of funding; likewise, do not submit a $50k report for $300k worth of funding. Include as many charts and figures as required to explain the work.